This is a peer-reviewed, author's accepted manuscript of the following research article: Adnan, M. S. G., Abdullah, A. Y. M., Dewan, A., & Hall, J. W.
The effects of changing land use and flood hazard on poverty in coastal Bangladesh.
Land Use Policy, 99, [104868].
https://doi.org/10.1016/j.landusepol.2020.104868

The effects of changing land use and flood hazard on poverty in coastal Bangladesh

Mohammed Sarfaraz Gani Adnan [a,b*], Abu Yousuf Md Abdullah [c], Ashraf Dewan [d], Jim W. Hall [a]

[a] Environmental Change Institute, School of Geography and the Environment, University of Oxford, South Parks Road, OX13QY Oxford, United Kingdom

[b] Department of Urban and Regional Planning, Chittagong University of Engineering and Technology (CUET), Chittagong 4349, Bangladesh

[c] School of Public Health and Health Systems, Faculty of Applied Health Sciences, University of Waterloo, Ontario, Canada

[d] Spatial Sciences Discipline, School of Earth and Planetary Sciences (EPS), Curtin University, Perth, Western Australia 6102, Australia

Abstract

The construction of polders in the coastal region of Bangladesh has significantly modified the patterns of flooding, as well as leading to significant land use/land cover (hereinafter, LULC) changes. The impact of LULC change and flooding on poverty is complex and poorly understood. This study presents a spatiotemporal appraisal of poverty in relation to LULC change and pluvial flood risk in the south western embanked area of Bangladesh. A combination of logistic regression (LR), cellular automata (CA), and Markov Chain models were utilised to predict future LULC based on historical data. Flood risk assessment was performed at present and for future LULC scenarios. A spatial regression model was developed, incorporating multiple parameters to estimate the wealth index (WI) for present-day and future scenarios. In the study area, agricultural lands reduced from 34% in 2005 to 8% in 2010, while aquaculture land cover increased from 17% to 39% during the same time. The rate of LULC change was relatively low between 2010 and 2019. Based on the recent trend, LULC was predicted for the year 2030. Flood risk was positively correlated with LULC and the expected annual damage (EAD) was estimated at $903 million in 2005, which is likely to increase to $2096 million by 2030, considering changes in LULC scenarios. The analysis further showed that the EAD and LULC change were negatively associated with the WI. Despite consistent national GDP growth in Bangladesh in recent years, the rate of increase of WI is likely to be low in the future because flood risk and patterns of LULC change have a negative effect on WI.

Key words: Land use change model; flood risk; poverty; Cellular Automata; Markov Chain

1. Introduction

It is widely recognised that poor people are disproportionately exposed to environmental hazards (Winsemius et al., 2018). There are several possible reasons for this. For instance, poor people tend to inhabit remote low-lying floodplains, due to the limited development opportunities and relatively cheaper lands (Dasgupta, 2007). Their livelihoods and assets are less protected (Bangalore et al., 2019; Hossain et al., 2012), and thus, they have relatively a low capacity to cope with property losses resulting from flooding (Brouwer et al., 2007).

Bangladesh is located in the floodplain of three major rivers — the Ganges, Brahmaputra, and Meghna. The combined discharge generated of these three rivers is the highest in the world. The peak run-off depth is also the highest, which, combined with storm surges generated from the Bay of Bengal. This makes a major portion of the country is prone to flooding (Dasgupta, 2007). Flood processes in the coastal region of Bangladesh are complex, as it can occur from multiple sources such as intense precipitation during the monsoon, high water levels in the rivers, and cyclone induced storm surges (Adnan et al., 2019). Different environmental stresses create biophysical and socioeconomic challenges in the coastal region. For instance, frequent flooding and increasing soil salinity limit agricultural productivity, which is the main source of livelihoods in coastal Bangladesh (Rahman et al., 2020).

Flood management approaches in the coastal region of Bangladesh include both structural and non-structural measures (Paul and Rashid, 2017; Rahman and Salehin, 2013). Major surge events induced by cyclones in the 1950s forced the then government to invest in the Coastal Embankment Project (CEP) in the 1960s. The CEP aimed at increasing agricultural production to ensure food security, by preventing salinity intrusion in the coastal region particularly during the dry season. As a part of the CEP, 139 polders (enclosed coastal embankments) were created in between the 1960s and 1980s (Islam et al., 2016; Warner et al., 2018). The construction of the polders has brought both beneficial and harmful effects on society and the environment. The protection from flooding afforded by embankments led to an increase in agricultural productivity until the 1980s (Adnan et al., 2020). Embankments have demonstrably protected the polder area against storm surges and fluvio-tidal floods of moderate severity (Adnan et al., 2019). However, the separation of floodplains from adjacent rivers caused geomorphological changes in the polder areas, exacerbating land subsidence inside polders (Auerbach et al., 2015). Accelerated land subsidence and inadequate drainage are accountable for frequent pluvial flooding (locally called 'waterlogging') (Adnan et al., 2019).

Generally, the construction of structural flood control measures, such as polders, shapes the pattern of human settlements and land use, which in turn impacts the extent of flood risk. Such flood control measures create the so-called "levee effect" (White, 1945). Whilst people tend to settle in less flood-prone areas, presence of structural flood defence system encourages floodplain development by engendering a sense of safety (Di Baldassarre et al., 2013; Montz and Tobin, 2008). Therefore, the failure of structural systems in the form of overtopping or breaching of embankments may exacerbate flood damages (Hui et al., 2016).

The pattern of land use/land cover (LULC) in the coastal region of Bangladesh has experienced major changes over the past half-century, following the construction of polders (Abdullah et al., 2019; Huq et al., 2015; Khan et al., 2015; Parvin et al., 2017; Rahman et al., 2017). Such changes largely occurred due to frequent and diverse natural hazards (e.g., floods) and increases in inundation, soil salinity, and land erosion (Brouwer et al., 2007; Khan et al., 2015). For instance, about 1% of agricultural land along the south western coast was transformed into non-agricultural use in each year over the past four decades due to the occurrence of frequent flooding (Rahman et al., 2017). The transformation of agricultural land to shrimp culture has been a common practice in the area since the 1980s as it can be more profitable (Khan et al., 2015). However, such land transformation has reportedly been leading to an increase in soil salinity, reducing agricultural production (Khan et al., 2015; Rahman et al., 2017).

Whilst anthropogenic drivers profoundly change the pattern of LULC, such transformation of land may affect local flooding processes (Wheater and Evans, 2009). The pattern of LULC determines the amount of runoff generated during a precipitation event, thus, influencing the water balance in an area. Hence, LULC may affect both the probability of flooding and its consequences (McColl and Aggett, 2007; Szwagrzyk et al., 2018). Flood losses are not only dependent on extreme hydro-meteorological conditions of a region, unplanned land use can multiply property damages (Lee and Brody, 2018). In coastal Bangladesh, unplanned LULC change may lead to environmental degradation such as soil salinization, disappearance of seasonal lagoons, and deterioration of water quality by increasing salinity (Islam et al., 2015).

Generally, flooding and poverty coexist particularly within rural communities, as damages caused by recurring flood events deplete assets, negatively impact agricultural incomes and thus lower quality of life of communities (Dube et al., 2018). It has been hypothesised that increasing flood risk and unplanned LULC change may create a poverty trap in the coastal region of Bangladesh (Ahmed, 2018; Borgomeo et al., 2017), inhibiting long-term development prospects (Parvin et al., 2017). Marginalised farmers could not generate adequate income through agricultural activities, whilst being unable to transform their agricultural land into aquaculture due to high cost associated with such change (Islam et al., 2015). As a result, they are unable to migrate out of such areas due to social and economic constraints and related costs (Dasgupta, 2007).

Regulating LULC change is an intervention to reduce flood risk, which has been adopted in different coastal cities (Adnan and Kreibich, 2016). Therefore, it is essential to understand the association between LULC and flood risk. Risk-based flood management approaches have received attention globally due to recent experience of several catastrophic events in many regions across the world (Hall et al., 2015; Hall et al., 2003b; Poussin et al., 2015), as well as the projected increase in the frequency and severity of flooding due to climate change-induced sea level rise (Koks, 2018). An empirical analysis of flood risk can support decision-makers to appraise and sequence investments for flood management (Dawson et al., 2011; Hall et al., 2003a; Hall et al., 2019; Hino and Hall, 2017; Sayers et al., 2002). The methods used in research and practice for quantifying flood hazard and vulnerability range from simple approaches (with numerous simplifying assumptions) to very complex applications, which are both data and time-intensive and computationally expensive (Apel et al., 2009; Dewan, 2013).

In the existing literature, the association between flood risk and poverty has been comprehended primarily by estimating exposure of poor people to flooding at various geographical scales (Bangalore et al., 2019; Brouwer et al., 2007; Qiang et al., 2017; Winsemius et al., 2018). In the case of coastal Bangladesh, a few studies have applied quantitative approaches (based on household survey data) to show how poverty exacerbates flood vulnerability/risk (Akter and Mallick, 2013; Brouwer et al., 2007). However, little is known about (i) how the pattern of LULC change influences flood risk at present and in the future; (ii) what is the association between LULC change and risk of flooding, and how they impact poverty spatially. We address these questions by estimating: (i) flood risk in relation to current and future LULC scenarios; and (ii) the change in poverty in relation to a change in LULC and flood risk.

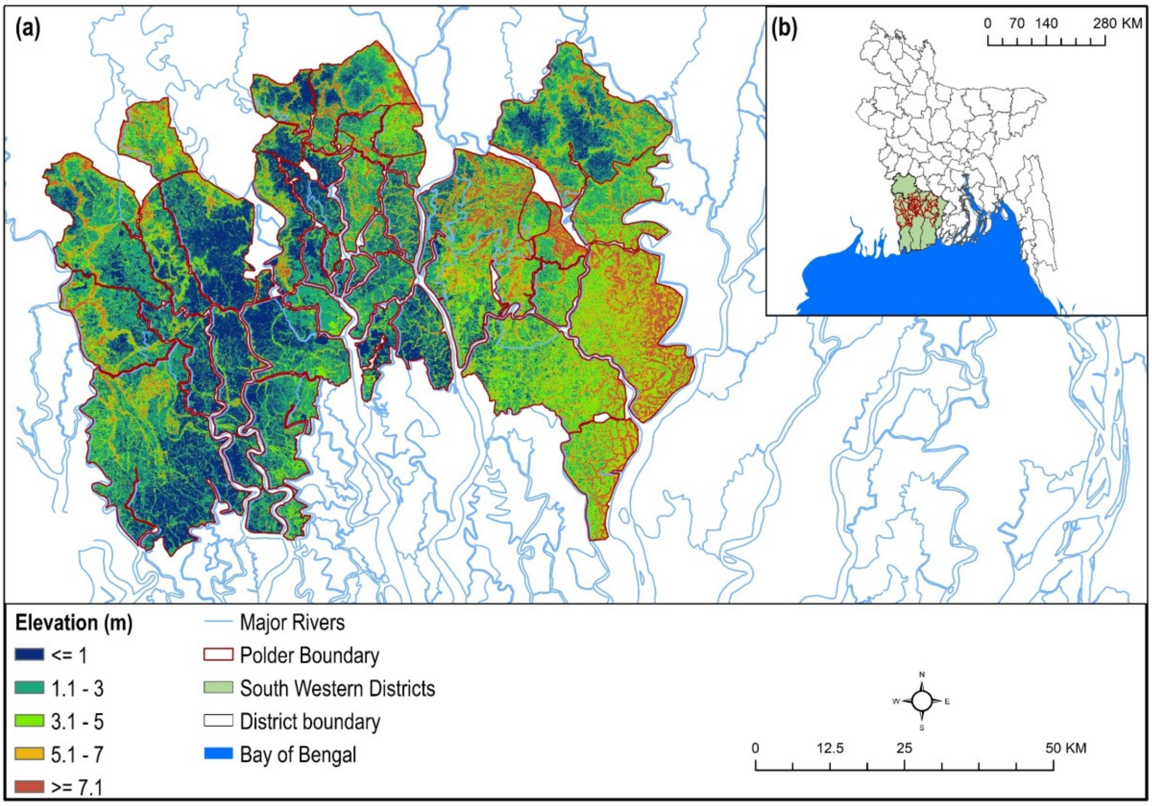

Figure 1 South western embanked area of Bangladesh

2. Materials and methods

This study was conducted in three stages. First, a model was established to analyse spatiotemporal patterns of LULC change and predict future LULC. Second, pluvial flood hazard was modelled to simulate the depth and extent of inundations for various return periods of monsoonal precipitation. Then flood risk was estimated at each LULC scenario (historical and future), for different flood return periods. Finally, a spatial regression model was developed to estimate poverty, incorporating geographical, environmental, and socio-economic parameters including LULC change and flood risk.

2.1. Description of the study area

This study focussed on polders in the south western coast of Bangladesh. The area includes a total of 44 polders, located in five coastal districts: Bagerhat, Jessore, Khulna, Pirojpur, and Satkhira (Figure 1). These polders were constructed to protect about 5187 km^2 of land, where approximately 5.3 million people live (WorldPop, 2018). The area has a mean elevation of 3.5 m and is heavily intersected by tidal rivers. The area is prone to three types of flooding — pluvial, fluvio-tidal, and surge floods. Inadequate drainage channels and increasing land subsidence exacerbate frequent pluvial flooding during the monsoon months (May to

September) (Adnan et al., 2019), when the area receives the maximum amount of precipitation (Figure 2). A lack of sedimentation and accelerated compaction within the embanked area led to a loss of 1.0-1.5 m elevation since the construction of polders in the 1960s (Auerbach et al., 2015). Agriculture, shrimp farming, and the natural resources of the Sundarban mangrove forest (located in the south of the study area) are the major sources of livelihoods and economy of the inhabitants (Khan et al., 2015). Approximately 80% of the total shrimp ponds of Bangladesh are located in south western coast (Ahmed, 2018). However, increased soil salinity resulting from the excessive shrimp farming has negatively impacted crop yield. The situation potentially affects the livelihoods of the poorest segments of society (Szabo et al., 2016). A risk-sensitive land use policy would help to alleviate the complex problems of the south western coast (Rahman et al., 2017). Thus, this study aimed to provide spatial information on land use change and flood risk, as well as their association with poverty.

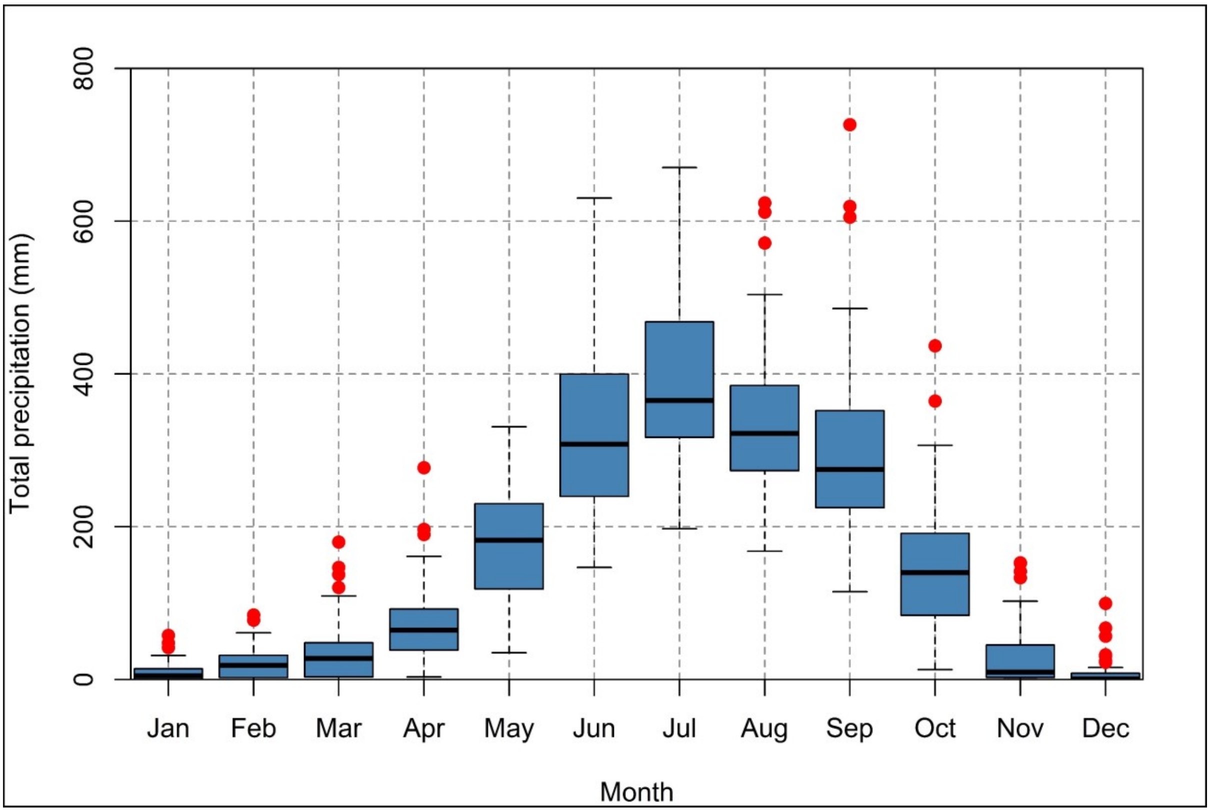

Figure 2 Box and whisker plot of monthly rainfall (1965-2012) for south western embanked area

2.2. Data

This study examined the effects of LULC change and flood risk on poverty. A range of spatial and hydrometeorological data were used to model LULC change, assess flood risk, and estimate poverty. A list of data is given in Table 1. The LULC dataset used in this study is an updated version of Abdullah et al. (2019). The dataset contains five classes: agricultural, aquaculture, bare land, built-up area (urban), vegetation with the rural settlement, and waterbody. The Advanced Land Observing Satellite (ALOS) digital elevation model (DEM) (JAXA, 2015) at 30 m resolution used to derive maps of various geomorphological parameters (e.g. elevation, slope, curvature) and establish flood hazard model. The ALOS DEM was used as it is considered to be highly reliable and freely available DEM, which has a low root mean square error (1.78m) in vertical accuracy (Adnan et al., 2020). Hydrometeorological data were collected from various organisations including Bangladesh Meteorological Department (BMD), Bangladesh Agricultural Research Council (BARC), and Water Resources Planning Organisation of Bangladesh (WARPO). This study considered the Wealth Index (WI) as an indicator of poverty. The WI data was obtained from Steele et al. (2017).

Table 1. Different data types used in this study

Data	**Description**	**Source**
1. LULC	LULC data of 2005, 2010, and 2019 at 30 m resolution	(Abdullah et al., 2019)
2. DEM	ALOS DEM of 30 m resolution	(JAXA, 2015)
3. Precipitation	Gridded (5km grid points) precipitation data of 10-day temporal resolution from 1965-2012	(www.bmd.gov.bd/)
4. Climate	Monthly average temperature, monthly average daylight hour data from 1988-2012, across four weather stations	(http://www.barc.gov.bd/)
5. Poverty	Gridded Demographic and Health Surveys (DHS) Wealth Index (WI)	(Steele et al., 2017)
6. Soil salinity	Gridded soil salinity index	(Abdullah et al., 2018)
7. Population density	Total number of people per 100 m grid-cell	(https://www.worldpop.org)
8. Gross Domestic Product (GDP)	Gridded GDP data of 30 arc-sec (~900m) resolution	(Kummu et al., 2018)
9. Agricultural employment	Number of people employed in the agricultural sector	(De Bono and Chatenoux, 2014)
10. Spatial data	GIS vector data of road network, river channels, and growth centre	(http://www.warpo.gov.bd)

2.3. Modelling LULC change

This study predicted LULC during 2030 using a combination of logistic regression (LR), cellular automata (CA), and Markov Chain models, following an approach by Arsanjani et al. (2013). A similar modelling approach has been used in several studies for detecting and simulating LULC change (Ahmed et al., 2013; Kityuttachai et al., 2013; Mitsova et al., 2011; Shahbazian et al., 2019; Wang et al., 2019). We applied this approach for following reasons: (i) it can incorporate both environmental and socio-economic variables; (ii) the model can incorporate a wide range of spatial factors; (iii) the LR model can use data at different scales; and (iv) the CA model can control spatial dynamics of LULC changes (Arsanjani et al., 2013; Shahbazian et al., 2019).

The CA model uses a principle that areas tend to change to a state based on the state of their neighbouring areas (Arsanjani et al., 2013). A CA system includes four components such as cells, states, neighbourhoods, and rules (Shahbazian et al., 2019). Cells are defined as the smallest unit and the state of each cell is determined by its initial state, the conditions in the surrounding cells, and a set of transition rules (Arsanjani et al., 2013; Verburg et al., 2004). The CA model in this study incorporated a LULC change map, transition potential maps created using LR models, the change rate calculated in the change analysis step, and a transition probability matrix predicted for a future year (using Markov Chain model).

2.3.1. Analysing LULC change

LULC data of 2005, 2010, and 2019 were analysed to detect spatiotemporal changes. The model initially calibrated LULC change over the period 2005-2010. While developing a LULC change map, the transition areas less than 5 km^2 (~0.001% of total area) were ignored, otherwise, the modelling approach would have been computationally expensive. As a result, the 2005-2010 change map included a total of 12 LULC transition categories.

2.3.2. Driving forces for detecting change

The LR models were established for all 12 transitions, to estimate the degree of influence of different factors (driving forces) on a type of LULC (Shahbazian et al., 2019). LULC changes could be governed by various combinations of geographical, environmental, and socio-economic factors (Dewan and Yamaguchi, 2009). Based on the knowledge attained from literature as well as expert knowledge on the study area, a total of 14 variables were selected (Table 2). For a LULC transition, the LR model incorporated a binary (change to a LULC class and no-change) dependent variable and different combinations of independent variables (driving forces). Combinations of independent variables were selected in a way that yielded the highest relative operating characteristic (ROC) and adjusted odds ratio values, indicating performance of the models (Arsanjani et al., 2013).

The LR model creates probability surface maps using the following equation (Hosmer Jr et al., 2013):

$$p = 1/(1 + e^{-z}) \tag{1}$$

where p ranges from 0 to 1 on an S-shaped curve, explaining the probability of a cell changing to a LULC class; z is the linear combination of independent variables (driving forces), which was estimated using the following equation:

$$z = b_0 + b_1x_1 + b_2x_2 + \cdots + b_nx_n \tag{2}$$

where b_0 is the model intercept, b_i (i = 1, 2, ..., n) indicates the coefficients of independent variables, and x_i (i = 1, 2, ..., n) represents the n number of independent variables.

2.3.3. Simulating future LULC

The CA-Markov Chain model was used to predict LULC change based on the estimated transition probabilities (Arsanjani et al., 2013; Shahbazian et al., 2019). The Markov Chain model predicted the quantity of change in each LULC transition. Based on the Bayes' theorem of conditional probability, LULC was predicted using the following formula (Sang et al., 2011):

$$S\,(t+1) = P_{ij} \times S(t) \tag{3}$$

where $S(t)$ and $S(t+1)$ are the LULC status at the time t and $t+1$, respectively; the transition probability matrix P_{ij} was estimated as follow:

$$P_{ij} = \begin{bmatrix} P_{11} & P_{12} & \cdots & P_{1n} \\ P_{21} & P_{22} & \cdots & P_{2n} \\ \cdots & \cdots & \cdots & \cdots \\ P_{n1} & P_{n2} & \cdots & P_{nn} \end{bmatrix}$$
$$\left(0 \leq P_{ij} < 1 \; and \; \sum_{j=1}^{n} P_{ij} = 1, (i, j = 1,2,3, \ldots n) \right) \tag{4}$$

where n is the total number of LULC classes. In this study, probability values of 2019 and 2030 were predicted based on transition matrices of 2005-2010 and 2010-2019, respectively. However, the spatial distribution of LULC in a Markov Chain model is unknown.

Therefore, the CA model was integrated to provide a spatial dimension to the model (Arsanjani et al., 2013; Corner et al., 2014; Shahbazian et al., 2019).

2.3.4. Validating the outputs

The LULC change model was validated for the year 2019. Therefore, considering LULC maps of 2005 and 2010 as the initial and final state maps, the model predicted LULC map of 2019. We compared predicted LULC map with observed data of 2019. Kappa statistic was estimated to determine the degree of agreement between observed and modelled LULC maps (Mitsova et al., 2011).

2.4.Flood risk assessment

Flood risk assessment was carried out for various LULC scenarios to estimate temporal changes of direct economic damage due to floods of various magnitudes. The risk was defined as the product of flood hazard, exposure, and vulnerability. The expected annual damages (EAD) at different LULC scenarios were estimated to represent spatiotemporal pattern of flood risk (Rojas et al., 2013).

2.4.1. Flood frequency analysis

This study primarily focused on pluvial flooding, considering increased frequency and severity of this type of flooding in the study area. Although historically, three types of flooding (pluvial, fluvio-tidal, and storm surge induced flooding) affect the study area, occurrence of pluvial flooding is a relatively recent and frequent phenomenon. Adnan et al. (2019) documented that monsoon precipitation caused inundation in the area every year from 1988 to 2012. Persistent pluvial flooding damages crops and therefore impacts the livelihoods of people who inhabit the south western coast (Alam et al., 2017).

Flood frequency analysis was carried out to estimate return periods of monsoon precipitation, which is the main source of pluvial flooding in the study area (Adnan et al., 2019). Seven recurrence intervals (i.e. 1, 2, 5, 10, 20, 50, and 100 years) of floods were considered here. Inundation depth was estimated at each cell within the study area. Since pluvial flood hazard model takes monthly precipitation as an input, we generated raster layers of monthly precipitation of seven return periods. To decide whether the climate in the near future (i.e. 2030) is likely to be in a ‘changed’ or ‘unchanged’ state, a precipitation trend analysis was performed. Therefore, linear regression models of monthly precipitation were established (Panda and Sahu, 2019). We also applied an autocorrelation function (ACF) to estimate whether monthly total precipitation was autocorrelated between years (Feng et al., 2016). No significant autocorrelation was found between successive years. The linear regression models confirmed the absence of a significant trend in monthly precipitation. The results of precipitation trend analysis are summarised in Table S3 and Figure S1 (see supplementary document). To generate monthly precipitation layers of seven return periods, extreme value analysis was conducted at each grid cell by fitting a generalized extreme-value (GEV) distribution using the L-moment method, following Adnan et al. (2019).

2.4.2. Flood hazard assessment

Flood hazard assessment included a hydrological simulation of floods of various return periods (Rojas et al., 2013). Inundation maps were also derived for seven recurrence intervals of monsoon precipitation — 1, 2, 5, 10, 20, 50, and 100 years — using a pluvial flood rainfall-runoff and spreading model established for the study area by Adnan et al. (2019). The modelling process started with estimating monthly water balance. A Thornthwaite and Mather water balance model was accompanied by the flood model, which estimated monthly excess precipitation at each grid cell, after subtracting evapotranspiration from monthly total precipitation. Monthly excess precipitation layers from May to September were aggregated to prepare excess precipitation layers during the monsoon. The inundation model incorporated the ALOS DEM to identify depressions and their catchments. During a flood event, the estimated total volume of excess precipitation was assigned to each depression according to the respective catchment position to represent both flood depth and extent. Further description of the model, validation process and sensitivity analysis can be found in Adnan et al. (2019). The flood hazard mapping resulted in inundation maps of seven recurrence intervals.

2.4.3. Flood vulnerability analysis

Flood vulnerability assessment generally includes the estimation of direct or indirect damages due to floods. Direct damages, which primarily occurred because of physical contact of houses, building, and public infrastructures with floodwater, are estimated as a function of flood depth in different cells, the relationship between flood depth and LULC (or structural use), and total cell area (Apel et al., 2009). Indirect damages can be an outcome of the failures of critical infrastructure systems, such as transportation, production, and energy (Koks et al., 2019). The scope of the study was however limited to estimating direct flood damages. It was estimated for three types of LULC (i.e. agriculture, aquaculture, and residential) using the following equation (Islam et al., 2019):

$$D_j = \left(\sum_{i=1}^{n} x_i \times f(x_i) \right) \times A \tag{5}$$

where D_j is the total damage (in million USD ($)) during a flood return period of j, x_i is the flood depth (m) in cell i, $f(x_i)$ is the damage function for the flood depth level x in cell i, and A is the area of a cell. Global depth-damage curves, adopted from Huizinga et al. (2017), were used to estimate direct tangible flood damage to residential and agricultural LULC. The depth-damage curve for aquaculture lands was obtained from Islam et al. (2019) (Figure 3). The maximum damage values in depth-damage functions were given in Euro, which we converted into USD using a currency conversion rate of 1 Euro = 1.11 USD.

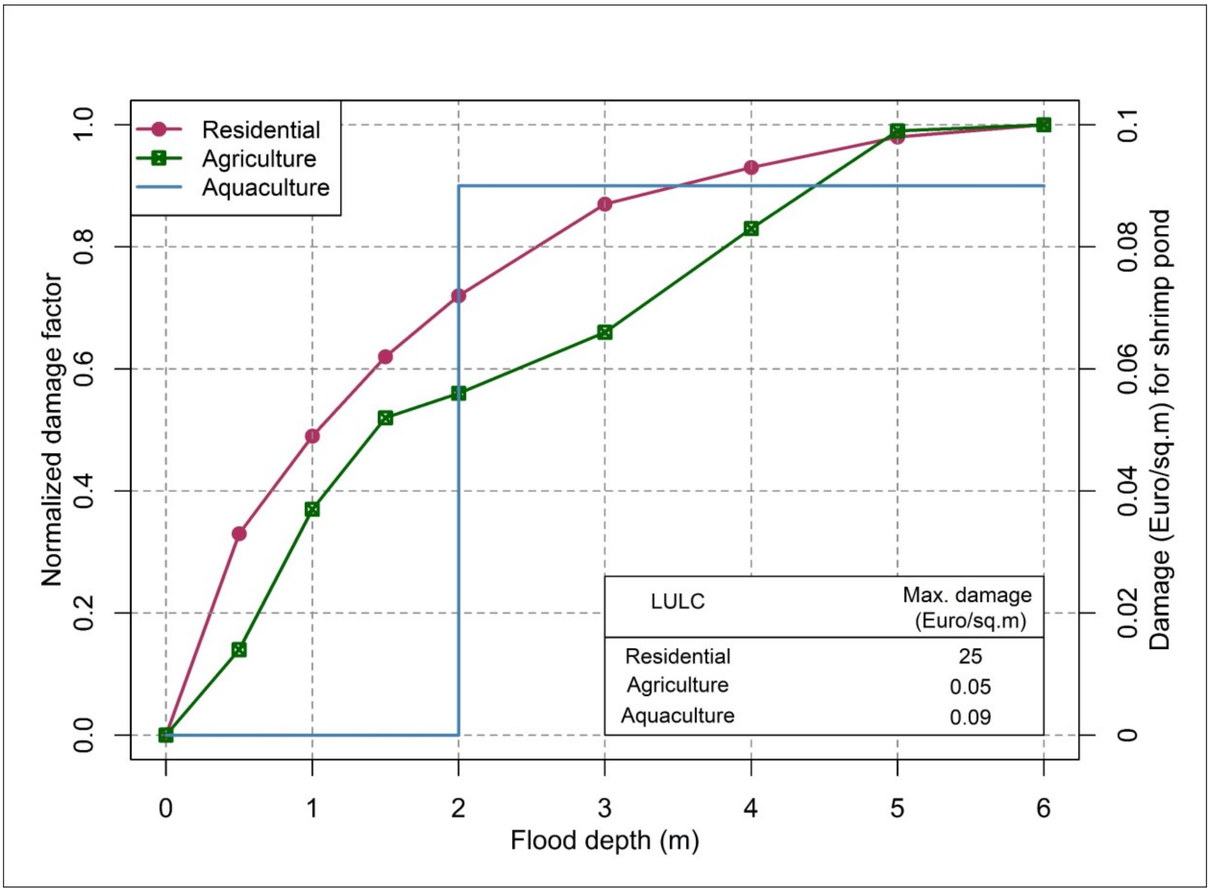

Figure 3 Depth-damage curves (adopted from Huizinga et al. (2017) and Islam et al. (2019))

Pixel-scale (30 m resolution) flood damage was estimated in a GIS for seven flood return periods (1, 2, 5, 10, 20, 50, and 100-year) at four LULC scenarios of 2005, 2010, 2019, and 2030. Inundation maps (see section 2.4.2) were overlaid on LULC maps to record flood depth and LULC according to each pixel. This dataset was imported in an R package and integrated with equation 5 to estimate pixel-scale flood damage, as well as total damage of the study area.

2.4.4. Estimating flood risk

Following flood hazard and vulnerability assessments, risks were estimated in the form of expected annual damage (EAD) for four LULC scenarios (2005, 2010, 2019, and 2030). The EAD can be estimated using the following equation (Olsen et al., 2015):

$$EAD = \iint_{A\,p} D(p)dpdA \tag{6}$$

where *D(p)* is the damage occurred during an event with the annual probability of exceedance *p* (approximated by the inverse of the flood return period (*T*)), *A* is the total area of the region under study. Since the choice of return periods influences flood risk estimates, a consideration of all return periods between the low and high probability floods enables an accurate estimation of risk (Ward et al., 2011). The probability space of flood risk for each integer year flood return period between 1 and 100 is discretised into 100 equal intervals, by interpolating flood damages estimated between seven recurrence intervals (Rojas et al., 2013). An exceedance probability curve was developed by plotting flood damages against corresponding exceedance probabilities. The exceedance probabilities of 0.01 (100-year) and 1 (1-year) were considered correspondingly as the lower and upper limits of the probability curve. The EAD was estimated as the area under the curve (AUC), applying the trapezoidal rule given in equation 7 (Olsen et al., 2015).

$$EAD = \frac{1}{2}\sum_{i=1}^{n}\left(\frac{1}{T_i} - \frac{1}{T_{i+1}}\right)(D_i + D_{i+1}) \tag{7}$$

where n is the total number of return periods which is 100; T_i is the return period of the i^{th} event; D_i is the estimated flood damage during the i^{th} event.

2.5. Downscaling poverty data

Flood damage may exacerbate the degree of poverty in a region, whilst poor people may be compelled to live in riskier locations (Dube et al., 2018). This study aimed at investigating the spatiotemporal distribution of poverty, diagnosing its association with flood risk and LULC change. Steele et al. (2017) developed a gridded poverty dataset for Bangladesh, combining data from multiple sources such as mobile phone, satellite, and traditional survey. The spatial scale of the database was determined by developing the service area coverage of a cellular network using the Voronoi polygons. The spatial resolution of the data varies from 60 m to 5 km, where poverty was represented as asset, consumption, and income-based measures of wellbeing. In this study, we considered the asset-based measure, i.e., Demographic and Health Surveys (DHS) Wealth Index (WI), because the WI yielded the highest accuracy of predictions than other poverty metrics (Steele et al., 2017). The WI is a measure of household's living standard that is calculated using survey data on household characteristics (e.g. material used for housing construction), ownership of selected assets (e.g., television, bicycles), and access to different facilities such as water supply and sanitation (https://www.dhsprogram.com). The values of the WI can be either positive or negative, where a higher value implies higher socioeconomic status (Steele et al., 2017).

We downscaled the gridded WI data obtained from Steele et al. (2017), establishing a GIS-based ordinary least square (OLS) model (equation 8) based on ten spatial parameters (Table 4). The south western embanked area is comprised of 303 Voronoi polygons. The polygons were used to extract the values of all parameters.

$$y = \beta_0 + \beta_1 X_1 + \beta_2 X_2 + \cdots + \beta_n X_n + \varepsilon \quad (8)$$

where y is the WI, X_n is the value n^{th} parameter, β is the regression coefficient, and ε is the random error in prediction or residuals.

Spatial parameters included soil salinity, elevation, EAD, relative flood frequency, distance from northing and easting coordinates, LULC change, population density, GDP, and the number of people employed in the agricultural sector. The selection of parameters was based on their (i) role in influencing poverty (ii) availability as gridded data. Soil salinity impacts poverty as increasing salinity in the coastal region hinders agricultural activity (Szabo et al., 2016). A map of relative flood frequency was collected from Adnan et al. (2020). To represent ground elevation, ALOS DEM was used. The EAD map developed in this study (see section 2.4.4) was included in the regression model. A binary (change or no-change) LULC change map from each previous time step was incorporated. Two layers, representing the Euclidean distance from northing and easting lines were produced, to understand the spatial distribution of WI. GDP indicates the extent of human and economic development of a country, may influence WI. Gridded GDP data was extracted for the study area from a global dataset developed by Kummu et al. (2018). The dataset has a spatial resolution of 30 arc-sec (~900m) and generated for years 1990, 2000, and 2015. Using the GDP data of 2015, we projected the GDP of 2010, 2019, and 2030, incorporating existing and projected GDP growth rates provided by the World Bank and the International Monetary Fund (IMF), respectively. Sources of gridded soil salinity, population density, and agricultural employment data are given in Table 1.

The year 2010 was considered as a base year for this analysis, as WI data was developed based on 2011 DHS and 2010 Household Income and Expenditure (HIES) survey data. Performance of the model was determined by estimating the coefficient of determination (R^2). The generated OLS regression equation was used to predict WI for the year 2019 and 2030. Therefore, four independent variables were adjusted accordingly: The EAD, LULC change, population density, and GDP, while other variables were assumed to be constant.

3. Results

3.1. LULC change modelling

3.1.1. Temporal change of LULC

Figure 4 (a) shows temporal changes of observed LULC from 2005 to 2019 and their spatial variations are presented in Figure S2 (see supplementary document). From 2005-2010, a significant decrease in agricultural land was observed, while the proportion of aquaculture category increased substantially. More than 50% of agricultural lands transformed into aquaculture use, with another 25% into rural settlements. Contrarily, LULC change from 2010-2019 was relatively stable, when the main transformation took place in bare land; about 23% bare land area transformed into rural settlements. Stable growth in rural and urban settlements was observed between the years 2005 and 2019.

3.1.2. Driving factors

Various combinations of geographical, environmental, and social factors account for different types of LULC transition. Table 2 shows regression coefficients of different factors influencing the transformation of agricultural lands into aquaculture, rural, and urban use within 2005-2010. The probability of LULC change from agricultural to aquaculture use is higher in areas characterised by low elevation, concave curvature, frequently affected by flooding, located in proximity to existing aquaculture lands, roads, and drainage channels, high level of soil salinity, and located in the northern portion of the study area. Notably, we found a positive correlation of flood frequency with LULC change from agriculture to rural and urban settlements. About 57% of the study area was inundated by at least two historical flood events from 1988 to 2012 (Adnan et al., 2020). Therefore, substantial development of the residential area took place in the flood-prone zones. A summary of LR models of the remaining nine LULC transitions is given in Table S1 of the supplementary document.

Table 2. Driving factors of LULC change from 2005 to 2010

Factors	Regression coefficient		
	Agriculture to aquaculture	Agriculture to rural settlement	Agriculture to built-up area (urban)
Intercept	1.41	1.25	9.53
Elevation	-0.02	0.11	-0.37
Slope	$-1e^{-04}$	$2e^{-05}$	$-2e^{-04}$
Curvature	0.05		
Flood frequency	0.69	0.19	0.43
Distance from aquaculture land	-0.34		
Distance from existing road	-0.04	-0.05	-0.06
Distance from residential area		-0.07	-2.42
Distance from adjacent river	-0.11		
Distance from drainage channel	-0.35		
Distance from growth centre		0.07	0.11
Soil salinity	0.39	0.25	
Distance from northing coordinates	-0.19	-0.31	-0.09
Distance from easting coordinates		-0.003	0.10
Population density	-0.21	0.05	0.18

The performance of each LR model is indicated by the estimated ROC and odds ratio (Table 3). A ROC value 1 indicates a perfect fit and ROC value 0.5 represents a random fit. Also, a higher adjusted odds ratio indicates a better performance of a model (Arsanjani et al., 2013). In this study, the LR model for LULC transformation from agriculture to aquaculture cover obtained highest estimates of these performance indicators.

Table 3. ROC and adjusted odds ratio values of LR models

*Transitions	ROC	Adjusted odds ratio
LULC -1 to LULC -2	0.93	81.27
LULC -1 to LULC -3	0.71	5.23
LULC -1 to LULC -4	0.91	24.67
LULC -1 to LULC -5	0.73	4.60
LULC -1 to LULC -6	0.89	17.82
LULC -2 to LULC -3	0.74	8.10
LULC -3 to LULC -1	0.67	4.28
LULC -3 to LULC -2	0.89	14.38
LULC -3 to LULC -5	0.68	2.96
LULC -5 to LULC -1	0.63	2.07
LULC -5 to LULC -2	0.93	35.74
LULC -5 to LULC -3	0.82	9.81

** LULC -1= Agriculture; LULC -2 = Aquaculture; LULC -3 = Bare land; LULC -4 = Built-up area (urban); LULC -5 = Vegetation with rural settlement; LULC -6 = Waterbody*

3.1.3. Predicting LULC

The combination of LR and CA-Markov chain model determined LULC quantitatively, where the LR model generated probability surfaces of different transitions, the Markov chain model predicted the quantity of change in each LULC transition, and the CA model controlled the spatial dynamics the projected LULC. The Markov chain model estimated the transition probability of 2030 based on the transition matrix 2010-2019 (Table S2, supplementary document). The simulation suggests that the proportion of agricultural land, bare land, and general waterbody is likely to decrease, while aquaculture lands, as well as rural and urban settlement areas, would increase (Figure 4a). In the case of the spatial distribution of different categories of LULC, aquaculture is likely to remain as the dominant type of LULC in northern and western segments of the study area given its economic return. Agricultural activities would mostly take place in the eastern segment, where "vegetation with rural settlement" is likely to be the dominant LULC category (Figure S2, supplementary document). The validation process yielded a kappa coefficient of 0.87, which indicates an acceptable degree of accuracy. However, the choice of driving forces affects the accuracy of the model (Wang et al., 2019). Although different environmental and socio-economic factors were considered in this study, a limited number of driving forces may have resulted in some errors in the predicted LULC.

3.2. Association between LULC change and flood risk

3.2.1. Flood damage

Flood damages are associated with the type of LULC in the study area. Figure 4 (b) shows estimated damages during floods of different recurrence intervals, under four LULC scenarios. An increasing trend of flood damages was estimated, with changes in recurrence intervals and LULC scenarios. The estimated average damage (across all recurrence intervals) of $1180 million in 2005 is likely to increase by the year 2030 to $2601 million. From 2005-2010, the highest increase of flood damage was estimated at $839 million for a flood event with a 50-year return period. Within this period, a significant transformation of LULC was observed, which resulted in a decrease in agriculture lands and an increase in aquaculture land (Figure 4 (a)).

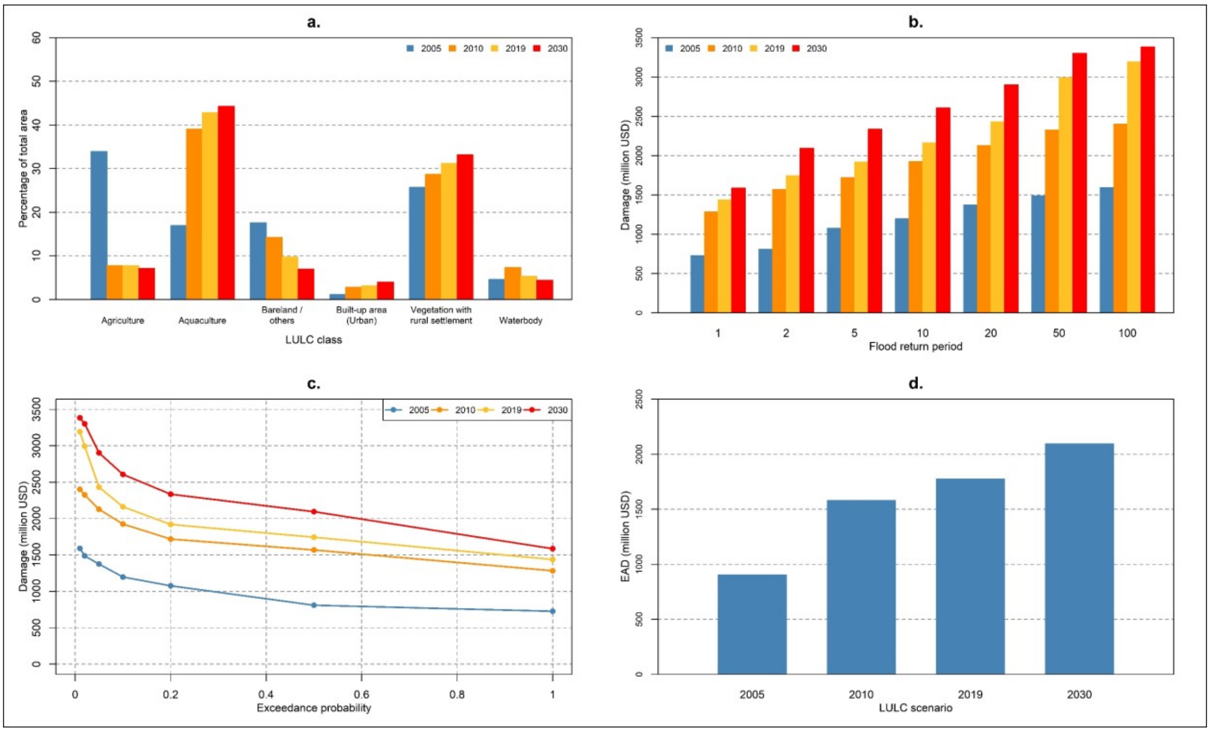

Figure 4 (a) Trend of LULC change from 2005 – 2030; (b) Estimated damages during floods of different return periods under four LULC scenarios; (c) Exceedance probability distribution curve; (d) Comparison of EAD among four LULC scenarios

3.2.2. Flood risk for various LULC scenarios

An exceedance probability curve in Figure 4 (c) and estimated EAD in Figure 4 (d) indicates contribution of LULC change to flood risk. Notably, in Figure 4 (c), the difference of flood losses between the highest and the lowest exceedance probabilities does not vary greatly. In 2005, damage of $809 million was estimated for the median annual maximum flood event (an event with a 2-year return period). The damage increased to $1591 million when the exceedance probability reduced to 0.01. In 2030, damages may range from $1586 million to $3384 million for floods with annual exceedance probabilities from 1 to 0.01, respectively. A relatively small difference in estimated damages between the low and high probability floods is because even frequent floods (e.g. the median annual maximum) cause a substantial extent of inundation, and thus, significant damages (Figure 4 (b)). With an increase in the magnitude of precipitation, depths in the inundated areas tend to increase substantially, rather than the extent of inundations. We estimate that the extent of inundation may range from 5% area (for the 2-year return period flood) to 15% area (for the 100-year flood).

LULC change has resulted in increased exposure primarily of residential (rural and urban) and aquaculture lands, which may result higher flood risk in the future. The EAD of the year 2005 was estimated to be approximately $903 million, which may be more than twice ($2096 million) by the year 2030 (Figure 4 (d)), assuming persistent LULC change in the future.

3.3. Association among LULC change, flood risk, and poverty

Table 4 summarises the results of the OLS regression model, developed to explain the degree of influence of different parameters on WI in the study area. Among the ten factors included, nine were found to be statistically significant. The estimated regression coefficients indicate that the WI was relatively higher in areas where land elevation, population density, and GDP are high, as well as a larger number of people employed in agriculture. Conversely, higher soil salinity, EAD, flood frequency, and LULC change negatively affected the WI. The regression coefficients were incorporated in Equation 8 in a GIS to estimate WI at each pixel, encompassing the study area. The estimated R^2 in Figure 6 (c) exhibits the performance of the model. The R^2 value of 0.81 indicates an acceptable level of agreement between observed versus modelled WI values for 2010.

Table 4. Estimated regression coefficients for downscaling wealth index (WI) data

Variables	**Coefficient**	**Standard error**	***t*-value**	**VIF**	***p*-value**
Intercept	-2.984	0.536	-5.572		0.000***
Soil salinity	-0.125	0.136	-0.925	2.70	0.317
Land elevation	0.042	0.009	4.472	3.08	$7e^{-06}$***
EAD	-0.016	0.007	-2.153	1.14	0.0373*
Relative flood frequency	-0.324	0.181	-1.791	1.81	0.059▪
Distance from northing coordinates	-0.132	0.018	-7.481	1.59	0.000***
Distance from easting coordinates	0.151	0.028	5.345	3.07	0.000***
LULC change	-0.213	0.091	-2.336	1.40	0.003**
Population density	0.182	0.012	14.754	1.68	0.000***
GDP	0.012	0.005	2.520	1.31	0.013*
Agricultural employment	0.298	0.039	7.342	1.40	0.000***
R^2: 0.81	Significance level: 0 '***' 0.001 '**' 0.01 '*' 0.05 '▪' 0.1 ' ' 1				

The WI of the study area was classified according to five categories using the Jenks scheme (Figure 5). During the base year of 2010, most of the south western zone (about 58%) was classified as areas with 'low' and 'very low' level of WI. Relatively, a higher WI was observed in the northern and western segments of the study area (Figure 5 (a)). The simulation showed a potential increase in WI in the year 2019 and 2030 (Figure 5 (b and c)). Figure S3 in the supplementary document compares the spatial distribution of WI in 2010 between the disaggregated data created in this study and the WI grid developed by Steele et al. (2017).

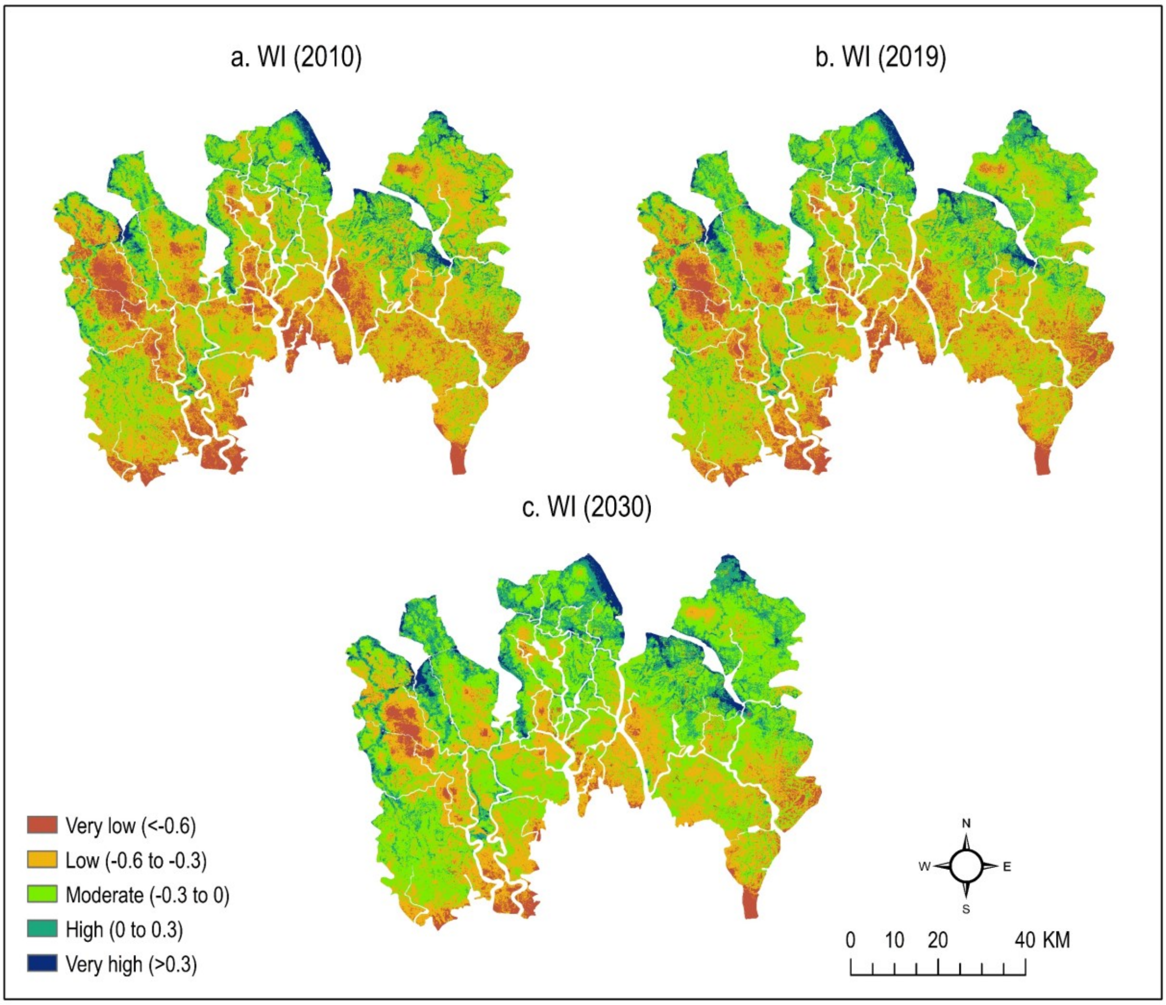

Figure 5 Spatiotemporal change of wealth index (WI) in the study area

Areas classified as 'very low' WI would potentially decrease from 15% area in 2010 to about 6% area in 2030, while the proportion of areas with 'moderate' WI may increase from 30% to 46%, respectively. However, the rate of increase in the proportion of areas classified as 'high' and 'very high' WI was estimated to be insignificant (Figure 6 (a)). The proportion of total area with positive WI ('high' and 'very high' categories) is likely to increase from 11% in 2010 to 18% in 2030. Bangladesh has an increasing GDP per capita growth, which was about 6.9% annually, on average, from 2010-2019. Population density has also been projected to increase in the future. Although these two variables exhibited a positive correlation with WI, LULC change and increasing EAD may hinder the growth of the WI in 2030. The estimated WI of 2010, 2019, and 2030 were disaggregated at the polder scale to identify marginalised polders at present and in future (Figure 6 (b)). In general, more than 50% of the total area in most of the polders were classified as zones with ‘low’ and ‘very low’ WI. In 2010, there were 19 polders where more than 50% area was classified as ‘moderate’ to ‘very high’. Nonetheless, the numbers increased in 2019 and 2030 for which correspondingly 21 and 34 polders were identified, with the majority of the area (>50%) classified as ‘moderate’ to ‘very high’ WI.

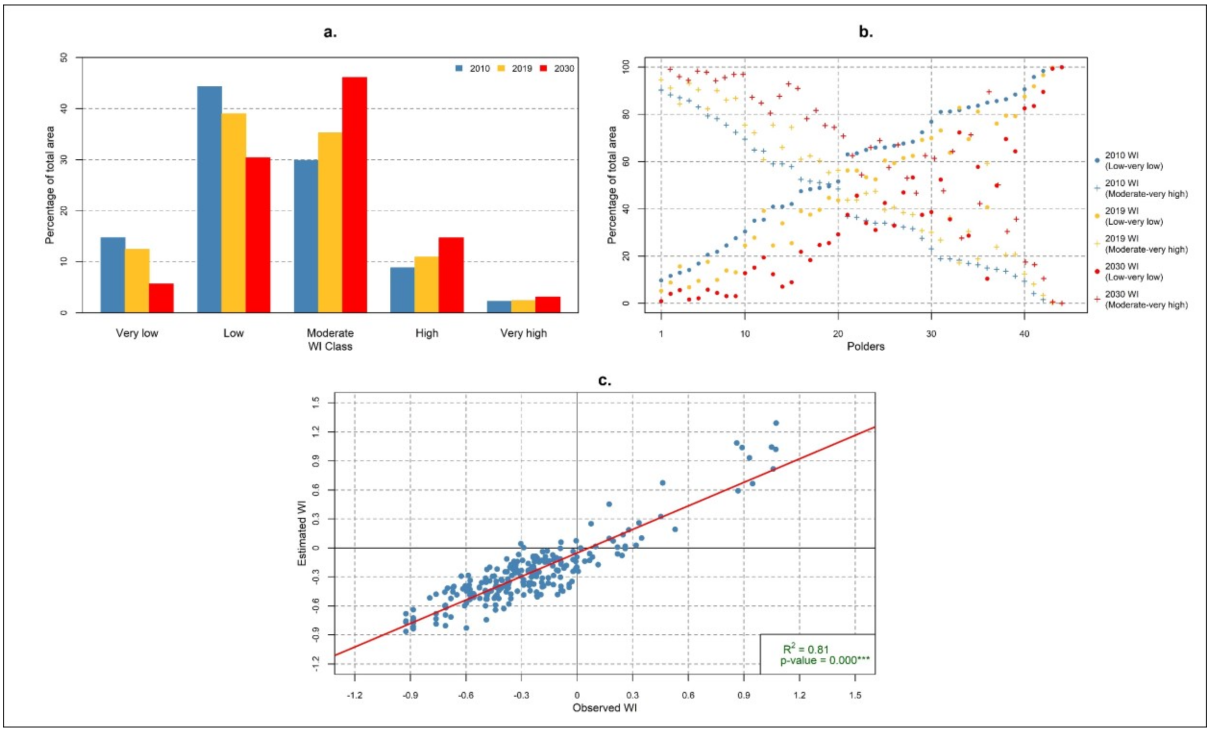

Figure 6 Temporal change of wealth index in: (a) South western embanked area and (b) Polders; (c) Association between observed and estimated WI in 2010

4. Discussion

Monitoring and managing LULC changes have been recognised as an essential geographic phenomenon for guiding socio-economic development (Corner et al., 2014; Shahbazian et al., 2019). This study analysed and simulated LULC changes in the south western embanked area of Bangladesh to understand their association with flood risk and poverty. The study results indicated that the proportion of agricultural lands decreased significantly between 2005 and 2019. This result is similar to a few other studies that focused on LULC changes in south western Bangladesh (Islam et al., 2015; Khan et al., 2015; Rahman et al., 2017). A significant reduction of agricultural lands is reportedly associated with growing prevalence of shrimp farming, which reflects a socio-economic trend whereby land-owners near existing shrimp farms are more likely to convert to shrimp, together with the effect of salinity intrusion, in particular following surge flood events, which forced farmers to transform their agricultural lands into aquaculture use (Islam et al., 2015; Khan et al., 2015). The projection of future LULC indicated a potential increase in settlement areas, while bare lands are likely to decrease. Such LULC transformation may follow a pattern which was observed from 2010-2019. Rahman et al. (2017) also predicted a similar pattern of LULC change by 2028 in a small administrative unit ('*upazila'*) of the south western coast. They explained that the natural increase of settlement and vegetation may lead to such changes in LULC.

Simulating future LULC is subject to uncertainty (Szwagrzyk et al., 2018). Although combined LR and CA-Markov Chain model considers a wide range of driving forces, it does not incorporate exogenous covariates such as personal preferences and government regulations (Arsanjani et al., 2013). For instance, lower market price, higher production cost, and increased frequency of diseases caused a decline in benefits in brackish water shrimp farming in the last decade (Akber et al., 2017). Although aquaculture was perceived as one of the few options for economic development (Akber et al., 2017), intensive aquaculture and subsequent salinity intrusion may result in poverty, promoting rural unemployment, social unrest, conflicts and forced migration (Johnson et al., 2016). Despite a reduction in brackish water shrimp cultivation in recent years, mixed cultivation of sweet water shrimp and fish has proved to be beneficial, which may persist in future. Therefore, in the current study, we considered the trend of LULC change in the last decade to predict future LULC. An alternative to the current LULC change model, an Agent Based Model (ABM) can incorporate individual-related factors, an approach which has been followed in recent studies to model LULC change (Arsanjani et al., 2013). However, the main limitation of the ABM is that it requires a large sample of empirical data to parameterise the model (Valbuena et al., 2010). In summary, LULC change modelling is a complex process and therefore, results should be used with caution (Wang et al., 2019). For example, areas predicted to be transformed into settlements by the LULC model should be interpreted as areas most suitable for future settlement development, rather than the precise locations of future change (Szwagrzyk et al., 2018).

Notably, this study found a positive association between LULC change and losses caused by floods for various recurrence intervals. A lack of risk-oriented residential development might be associated with increased flood risk. The majority of rural houses are temporary or semi-permanent structures (Akter and Mallick, 2013). Exposure of those areas to floods results in significant damages. Similar evidence of residential development in wetlands in recent years can be found in the existing literature (Akber et al., 2018). Aquaculture lands, comprised of shrimp or freshwater ponds, can withstand a certain depth of floodwater (i.e. < 2 m). However, when the depth increases, shrimp or fish may escape and cause financial losses (Islam et al., 2019).

We found that pluvial floods that occur each year cause substantial damage in the south western embanked region. This more or less inevitable flood damage is attributed to geomorphological characteristics of the study area. Land subsidence in the embanked region created depressions, which are prone to frequent pluvial flooding. Therefore, annual monsoon precipitation causes a substantial extent of inundation. For instance, a monsoon precipitation event of 2.1-year return period in 1990 inundated about 9.3% of the total area (Adnan et al., 2019). From 2009-2014, pluvial flooding in Khulna Division (where the study area located) caused greater damage than any other natural hazards (BBS, 2015). Frequent pluvial flooding in the south western embanked region causes both damages to crops and delay to winter crop cultivation (Alam et al., 2017).

This study further presented a spatially explicit regression model to estimate poverty in terms of the WI. The results indicated a positive correlation of GDP and population density with the WI. A similar pattern of association of these parameters with poverty was reported elsewhere (Dasgupta, 2007). The results of poverty modelling in this work highlighted that the rate of increase of WI is likely to be low in the future because of the pattern of LULC change and associated increase in flood risk. Few other studies have quantified the association between poverty indicators and flood risk/vulnerability (Akter and Mallick, 2013; Brouwer et al., 2007). Those studies were based on household-level survey data, where poverty was considered as an indicator of flood risk.

5. Conclusion

This study quantified the degree of influence of LULC change and flood risk on poverty in the south western embanked area of Bangladesh. Poverty was estimated, in terms of WI, for the present-day and for future LULC and flood risk scenarios. The analysis indicated that the region has been experiencing a rapid LULC change, resulting in a significant decrease in agricultural lands, while the proportion of aquaculture lands increased consequently. Based on the recent pattern of changes, LULC was predicted for the year 2030. The study further demonstrated that losses due to floods of various recurrence intervals have increased with LULC change. The exposure of residential areas (rural and urban) was predicted to increase in future. A lack of attention to flood is risk in land development decisions may explain the increased flood loss. Likewise, the expected annual flood damage (EAD) was also estimated to increase in the future LULC scenario. Moreover, we further estimated that LULC change and EAD negatively influence WI, which may restrict the growth of the WI in the future. The area with negative WI is predicted to decrease from 89% area in 2010 to 82% area in 2030, which is slower than one might expect given Bangladesh's predicted GDP growth. This is because flood risk and patterns of LULC change have a negative effect on WI. Among 44 polders analysed, more than 50% area in 11 polders would potentially have 'low' and 'very low' WI.

When interpreting the findings of this study, uncertainty related to flood damage functions and values of input parameters for poverty estimation should be considered. We considered global flood depth-damage functions for different LULC, due to the unavailability of micro (local)-level functions. We estimated flood losses for different categories of LULC, as building-level land use data are not available for all of the study area. While describing uncertainty in flood depth-damage function, Huizinga et al. (2017) highlighted that materials of structures primarily determine the maximum damage that may occur during a flood. In this study, the accuracy of the projected WI depends on the accuracy of input parameters. Parameters value (e.g. soil salinity and flood frequency) which were assumed to remain constant in may change in the future. The dynamics in soil salinity may also change in future climate change scenarios. Although few studies focused on modelling soil salinity in coastal Bangladesh under future climate change scenario (Dasgupta et al., 2015; Payo et al., 2017), the coarser resolution of their results restricted this study to incorporate such data in estimating WI. However, the statistical significance of salinity remains low. Also, GDP and population density were projected for the future year considering national-level growth rates, which may vary at the local scale such as polder level.

This study highlights that the absence of risk-oriented land use planning is potentially increasing flood risk in the coastal region. Various national and regional level policies of Bangladesh have addressed this issue and express the need to formulate land use plans following a risk-based approach. For instance, the Coastal Development Strategy focused on developing a coastal land use plan. More recently, the Bangladesh Delta Plan (BDP) 2100 emphasised the adoption of measures to mitigate flood risk, to achieve a long-term goal of reducing poverty and ensuring sustainable livelihoods (Khan, 2018). Spatial information on flood risk and land use changes provided in this study should inform stakeholders such as the Ministry of Land in identifying areas required land use policy intervention. Also, the proposed methodology to assess the implications of changing land use and flood risk for poverty should be of interest to land use planners. The results can help target policies in areas with greater poverty at present and in future scenarios. To the best of our knowledge, this study is the first attempt to model spatiotemporal change of poverty with changes in land use and flood risk. Although many studies focused on land use change modelling and/or flood risk assessment, there is a dearth of studies that quantify their combined influence on local level poverty.

Acknowledgement

This work is an output from the REACH programme (www.reachwater.org.uk) funded by UK Aid from the UK Department for International Development (DFID) for the benefit of developing countries (Aries Code 201880). However, the views expressed, and information contained in it are not necessarily those of or endorsed by DFID, which can accept no responsibility for such views or information, or reliance placed on them.

6. Reference

Abdullah, A.Y.M., Biswas, R.K., Chowdhury, A.I., Billah, S.M., 2018. Modeling soil salinity using direct and indirect measurement techniques: A comparative analysis. Environmental Development 29, 67-80.

Abdullah, A.Y.M., Masrur, A., Adnan, M.S.G., Baky, M.A.A., Hassan, Q.K., Dewan, A., 2019. Spatio-Temporal Patterns of Land Use/Land Cover Change in the Heterogeneous Coastal Region of Bangladesh between 1990 and 2017. Remote Sensing 11, 790.

Adnan, M.S.G., Haque, A., Hall, J.W., 2019. Have coastal embankments reduced flooding in Bangladesh? Science of the Total Environment 682, 405-416.

Adnan, M.S.G., Talchabhadel, R., Nakagawa, H., Hall, J.W., 2020. The potential of Tidal River Management for flood alleviation in South Western Bangladesh. Science of The Total Environment 731, 138747.

Adnan, S.G., Kreibich, H., 2016. An evaluation of disaster risk reduction (DRR) approaches for coastal delta cities: a comparative analysis. Natural Hazards 83, 1257-1278.

Ahmed, B., Kamruzzaman, M., Zhu, X., Rahman, M., Choi, K., 2013. Simulating land cover changes and their impacts on land surface temperature in Dhaka, Bangladesh. Remote Sensing 5, 5969-5998.

Ahmed, S., 2018. Shrimp farming at the interface of land use change and marginalization of local farmers: critical insights from southwest coastal Bangladesh. Journal of land use science 13, 251-258.

Akber, M.A., Islam, M.A., Ahmed, M., Rahman, M.M., Rahman, M.R., 2017. Changes of shrimp farming in southwest coastal Bangladesh. Aquaculture International 25, 1883-1899.

Akber, M.A., Khan, M.W.R., Islam, M.A., Rahman, M.M., Rahman, M.R., 2018. Impact of land use change on ecosystem services of southwest coastal Bangladesh. Journal of Land Use Science 13, 238-250.

Akter, S., Mallick, B., 2013. The poverty–vulnerability–resilience nexus: Evidence from Bangladesh. Ecological Economics 96, 114-124.

Alam, M.S., Sasaki, N., Datta, A., 2017. Waterlogging, crop damage and adaptation interventions in the coastal region of Bangladesh: A perception analysis of local people. Environmental Development 23, 22-32.

Apel, H., Aronica, G.T., Kreibich, H., Thieken, A.H., 2009. Flood risk analyses - How detailed do we need to be? Natural Hazards 49, 79-98.

Arsanjani, J.J., Helbich, M., Kainz, W., Boloorani, A.D., 2013. Integration of logistic regression, Markov chain and cellular automata models to simulate urban expansion. International Journal of Applied Earth Observation and Geoinformation 21, 265-275.

Auerbach, L.W., Goodbred, S.L., Jr., Mondal, D.R., Wilson, C.A., Ahmed, K.R., Roy, K., Steckler, M.S., Small, C., Gilligan, J.M., Ackerly, B.A., 2015. Flood risk of natural and embanked landscapes on the Ganges-Brahmaputra tidal delta plain. Nature Climate Change 5, 153-157.

Bangalore, M., Smith, A., Veldkamp, T., 2019. Exposure to Floods, Climate Change, and Poverty in Vietnam. Economics of Disasters and Climate Change 3, 79-99.

BBS, 2015. Bangladesh Disaster-related Statistics 2015. Climate Change and Natural Disaster Perspectives Bangladesh Bureau of Statistics (BBS), Ministry of Planning, Dhaka, Bangladesh.

Borgomeo, E., Hall, J.W., Salehin, M., 2017. Avoiding the water-poverty trap: insights from a conceptual human-water dynamical model for coastal Bangladesh. International Journal of Water Resources Development, 1-23.

Brouwer, R., Akter, S., Brander, L., Haque, E., 2007. Socioeconomic Vulnerability and Adaptation to Environmental Risk: A Case Study of Climate Change and Flooding in Bangladesh. Risk Analysis 27, 313-326.

Corner, R.J., Dewan, A.M., Chakma, S., 2014. Monitoring and prediction of land-use and land-cover (LULC) change, Dhaka megacity. Springer, pp. 75-97.

Dasgupta, A., 2007. Floods and poverty traps: Evidence from Bangladesh. Economic and Political Weekly, 3166-3171.

Dasgupta, S., Hossain, M.M., Huq, M., Wheeler, D., 2015. Climate change and soil salinity: The case of coastal Bangladesh. Ambio 44, 815-826.

Dawson, R.J., Ball, T., Werritty, J., Werritty, A., Hall, J.W., Roche, N., 2011. Assessing the effectiveness of non-structural flood management measures in the Thames Estuary under conditions of socio-economic and environmental change. Global Environmental Change 21, 628-646.

De Bono, A., Chatenoux, B., 2014. A global exposure model for GAR 2015, The Global Assessment Report on Disaster Risk Reduction 2015. United Nations Office for Disaster Risk Reduction (UNISDR), Geneva.

Dewan, A., 2013. Floods in a megacity: geospatial techniques in assessing hazards, risk and vulnerability. Springer.

Dewan, A.M., Yamaguchi, Y., 2009. Land use and land cover change in Greater Dhaka, Bangladesh: Using remote sensing to promote sustainable urbanization. Applied geography 29, 390-401.

Di Baldassarre, G., Viglione, A., Carr, G., Kuil, L., Salinas, J.L., Blöschl, G., 2013. Socio-hydrology: conceptualising human-flood interactions. Hydrol. Earth Syst. Sci. 17, 3295-3303.

Dube, E., Mtapuri, O., Matunhu, J., 2018. Flooding and poverty: Two interrelated social problems impacting rural development in Tsholotsho district of Matabeleland North province in Zimbabwe. Jàmbá: Journal of Disaster Risk Studies 10, 1-7.

Feng, G., Cobb, S., Abdo, Z., Fisher, D.K., Ouyang, Y., Adeli, A., Jenkins, J.N., 2016. Trend analysis and forecast of precipitation, reference evapotranspiration, and rainfall deficit in the Blackland Prairie of Eastern Mississippi. Journal of Applied Meteorology and Climatology 55, 1425-1439.

Hall, J.W., Berkhout, F., Douglas, R., 2015. Responding to adaptation emergencies. Nature Climate Change 5, 6-7.

Hall, J.W., Dawson, R.J., Sayers, P.B., Rosu, C., Chatterton, J.B., Deakin, R., 2003a. A methodology for national-scale flood risk assessment. Proceedings of the Institution of Civil Engineers: Water and Maritime Engineering 156, 235-247.
Hall, J.W., Harvey, H., Manning, L.J., 2019. Adaptation thresholds and pathways for tidal flood risk management in London. Climate Risk Management 24, 42-58.
Hall, J.W., Meadowcroft, I.C., Sayers, P.B., Bramley, M.E., 2003b. Integrated Flood Risk Management in England and Wales. Natural Hazards Review 4, 126-135.
Hino, M., Hall, J.W., 2017. Real options analysis of adaptation to changing flood risk: Structural and nonstructural measures. ASCE-ASME Journal of Risk and Uncertainty in Engineering Systems, Part A: Civil Engineering 3, 04017005.
Hosmer Jr, D.W., Lemeshow, S., Sturdivant, R.X., 2013. Applied logistic regression. John Wiley & Sons.
Hossain, M.A., Reza, M.I., Rahman, S., Kayes, I., 2012. Climate Change and its Impacts on the Livelihoods of the Vulnerable People in the Southwestern Coastal Zone in Bangladesh, in: Leal Filho, W. (Ed.), Climate Change and the Sustainable Use of Water Resources. Springer Berlin Heidelberg, Berlin, Heidelberg, pp. 237-259.
Hui, R., Jachens, E., Lund, J., 2016. Risk-based planning analysis for a single levee. Water Resources Research 52, 2513-2528.
Huizinga, J., de Moel, H., Szewczyk, W., 2017. Global flood depth-damage functions: Methodology and the database with guidelines. Joint Research Centre (Seville site).
Huq, N., Hugé, J., Boon, E., Gain, A., 2015. Climate change impacts in agricultural communities in rural areas of coastal Bangladesh: a tale of many stories. Sustainability 7, 8437-8460.
Islam, G.M.T., Islam, A.K.M.S., Shopan, A.A., Rahman, M.M., Lázár, A.N., Mukhopadhyay, A., 2015. Implications of agricultural land use change to ecosystem services in the Ganges delta. Journal of Environmental Management 161, 443-452.
Islam, M.A., Mitra, D., Dewan, A., Akhter, S.H., 2016. Coastal multi-hazard vulnerability assessment along the Ganges deltaic coast of Bangladesh–A geospatial approach. Ocean & Coastal Management 127, 1-15.
Islam, M.F., Bhattacharya, B., Popescu, I., 2019. Flood risk assessment due to cyclone-induced dike breaching in coastal areas of Bangladesh. Natural Hazards and Earth System Sciences 19, 353-368.
JAXA, 2015. ALOS global digital surface model “ALOS world 3D-30m (AW3D30)”. Japan Aerospace Exploration Agency (JAXA).
Johnson, F.A., Hutton, C.W., Hornby, D., Lázár, A.N., Mukhopadhyay, A., 2016. Is shrimp farming a successful adaptation to salinity intrusion? A geospatial associative analysis of poverty in the populous Ganges–Brahmaputra–Meghna Delta of Bangladesh. Sustainability Science 11, 423-439.
Khan, M.M.H., Bryceson, I., Kolivras, K.N., Faruque, F., Rahman, M.M., Haque, U., 2015. Natural disasters and land-use/land-cover change in the southwest coastal areas of Bangladesh. Regional Environmental Change 15, 241-250.
Khan, Z.H., 2018. Bangladesh Delta Plan 2100 - Baseline Studies on Water Resources Management (Coast and Polder Issues), in: Alam, S., Heer, J.d., Choudhury, G. (Eds.). General Economics Division (GED), Bangladesh Planning Commission, Dhaka, Bangladesh.
Kityuttachai, K., Tripathi, N., Tipdecho, T., Shrestha, R., 2013. CA-Markov analysis of constrained coastal urban growth modeling: Hua Hin seaside city, Thailand. Sustainability 5, 1480-1500.
Koks, E., 2018. Moving flood risk modelling forwards. Nature Climate Change 8, 561-562.

Koks, E., Pant, R., Thacker, S., Hall, J.W., 2019. Understanding Business Disruption and Economic Losses Due to Electricity Failures and Flooding. International Journal of Disaster Risk Science.
Kummu, M., Taka, M., Guillaume, J.H., 2018. Gridded global datasets for gross domestic product and Human Development Index over 1990–2015. Scientific data 5, 180004.
Lee, Y., Brody, S.D., 2018. Examining the impact of land use on flood losses in Seoul, Korea. Land use policy 70, 500-509.
McColl, C., Aggett, G., 2007. Land-use forecasting and hydrologic model integration for improved land-use decision support. Journal of Environmental Management 84, 494-512.
Mitsova, D., Shuster, W., Wang, X., 2011. A cellular automata model of land cover change to integrate urban growth with open space conservation. Landscape and Urban Planning 99, 141-153.
Montz, B.E., Tobin, G.A., 2008. Livin'large with levees: Lessons learned and lost. Natural Hazards Review 9, 150-157.
Olsen, A., Zhou, Q., Linde, J., Arnbjerg-Nielsen, K., 2015. Comparing methods of calculating expected annual damage in urban pluvial flood risk assessments. Water 7, 255-270.
Panda, A., Sahu, N., 2019. Trend analysis of seasonal rainfall and temperature pattern in Kalahandi, Bolangir and Koraput districts of Odisha, India. Atmospheric Science Letters 20, e932.
Parvin, G.A., Ali, M.H., Fujita, K., Abedin, M.A., Habiba, U., Shaw, R., 2017. Land use change in southwestern coastal Bangladesh: Consequence to food and water supply, Land use management in disaster risk reduction. Springer, pp. 381-401.
Paul, B.K., Rashid, H., 2017. Climatic Hazards In Coastal Bangladesh - Non-Structural and Structural Solutions, I ed. Elsevier, Cambridge, United States, 342 pp.
Payo, A., Lázár, A.N., Clarke, D., Nicholls, R.J., Bricheno, L., Mashfiqus, S., Haque, A., 2017. Modeling daily soil salinity dynamics in response to agricultural and environmental changes in coastal Bangladesh. Earth's Future 5, 495-514.
Poussin, J.K., Botzen, W.W., Aerts, J.C., 2015. Effectiveness of flood damage mitigation measures: Empirical evidence from French flood disasters. Global Environmental Change 31, 74-84.
Qiang, Y., Lam, N.S.N., Cai, H., Zou, L., 2017. Changes in Exposure to Flood Hazards in the United States. Annals of the American Association of Geographers 107, 1332-1350.
Rahman, M.M., Ghosh, T., Salehin, M., Ghosh, A., Haque, A., Hossain, M.A., Das, S., Hazra, S., Islam, N., Sarker, M.H., 2020. Ganges-Brahmaputra-Meghna Delta, Bangladesh and India: A Transnational Mega-Delta, Deltas in the Anthropocene. Springer, pp. 23-51.
Rahman, M.T.U., Tabassum, F., Rasheduzzaman, M., Saba, H., Sarkar, L., Ferdous, J., Uddin, S.Z., Zahedul Islam, A.Z.M., 2017. Temporal dynamics of land use/land cover change and its prediction using CA-ANN model for southwestern coastal Bangladesh. Environmental Monitoring and Assessment 189, 565.
Rahman, R., Salehin, M., 2013. Flood Risks and Reduction Approaches in Bangladesh, in: Shaw, R., Mallick, F., Islam, A. (Eds.), Disaster Risk Reduction Approaches in Bangladesh. Springer, Tokyo, pp. 65-90.
Rojas, R., Feyen, L., Watkiss, P., 2013. Climate change and river floods in the European Union: Socio-economic consequences and the costs and benefits of adaptation. Global Environmental Change 23, 1737-1751.
Sang, L., Zhang, C., Yang, J., Zhu, D., Yun, W., 2011. Simulation of land use spatial pattern of towns and villages based on CA–Markov model. Mathematical and Computer Modelling 54, 938-943.

Sayers, P.B., Hall, J.W., Meadowcroft, I.C., 2002. Towards risk-based flood hazard management in the UK. Proceedings of the Institution of Civil Engineers: Civil Engineering 150, 36-42.

Shahbazian, Z., Faramarzi, M., Rostami, N., Mahdizadeh, H., 2019. Integrating logistic regression and cellular automata–Markov models with the experts' perceptions for detecting and simulating land use changes and their driving forces. Environmental monitoring and assessment 191, 422.

Steele, J.E., Sundsøy, P.R., Pezzulo, C., Alegana, V.A., Bird, T.J., Blumenstock, J., Bjelland, J., Engø-Monsen, K., de Montjoye, Y.-A., Iqbal, A.M., 2017. Mapping poverty using mobile phone and satellite data. Journal of The Royal Society Interface 14, 20160690.

Szabo, S., Hossain, M.S., Adger, W.N., Matthews, Z., Ahmed, S., Lázár, A.N., Ahmad, S., 2016. Soil salinity, household wealth and food insecurity in tropical deltas: evidence from south-west coast of Bangladesh. Sustainability Science 11, 411-421.

Szwagrzyk, M., Kaim, D., Price, B., Wypych, A., Grabska, E., Kozak, J., 2018. Impact of forecasted land use changes on flood risk in the Polish Carpathians. Natural Hazards 94, 227-240.

Valbuena, D., Verburg, P.H., Bregt, A.K., Ligtenberg, A., 2010. An agent-based approach to model land-use change at a regional scale. Landscape ecology 25, 185-199.

Verburg, P.H., Schot, P.P., Dijst, M.J., Veldkamp, A., 2004. Land use change modelling: current practice and research priorities. GeoJournal 61, 309-324.

Wang, M., Cai, L., Xu, H., Zhao, S., 2019. Predicting land use changes in northern China using logistic regression, cellular automata, and a Markov model. Arabian Journal of Geosciences 12, 790.

Ward, P.J., De Moel, H., Aerts, J., Glade, T., 2011. How are flood risk estimates affected by the choice of return-periods? Natural Hazards & Earth System Sciences 11.

Warner, J.F., van Staveren, M.F., van Tatenhove, J., 2018. Cutting dikes, cutting ties? Reintroducing flood dynamics in coastal polders in Bangladesh and the netherlands. International Journal of Disaster Risk Reduction 32, 106-112.

Wheater, H., Evans, E., 2009. Land use, water management and future flood risk. Land use policy 26, S251-S264.

White, G.F., 1945. Human adjustment to floods, Department of Geography The University of Chicago, Chicago.

Winsemius, H.C., Jongman, B., Veldkamp, T.I.E., Hallegatte, S., Bangalore, M., Ward, P.J., 2018. Disaster risk, climate change, and poverty: assessing the global exposure of poor people to floods and droughts. Environment and Development Economics 23, 328-348.

WorldPop, 2018. Bangladesh 100m Population, Version 2, in: Southampton, U.o. (Ed.), UK.

The effects of changing land use and flood hazard on poverty in coastal Bangladesh

Supplementary tables

Table S1. Influence of driving forces on LULC change

Factors	**LULC 1 to LULC 3**	**LULC 1 to LULC 6**	**LULC 2 to LULC 3**	**LULC 3 to LULC 1**	**LULC 3 to LULC 2**	**LULC 3 to LULC 5**	**LULC 5 to LULC 1**	**LULC 5 to LULC 2**	**LULC 5 to LULC 3**
Intercept	2.38	-2.01	-0.57	-3.92	-5.86	-1.35	0.50	-1.51	2.14
Elevation	-0.32	-0.49	-0.03	0.32	0.03	0.10	-0.10	-0.51	-0.63
Curvature		0.39		-0.20	-0.01	-0.03			
Flood frequency	0.01	0.79	-0.41	0.13	0.72	0.17	-0.22	0.61	-0.18
Distance from aquaculture land								-0.10	
Distance from existing road	-0.06			0.08		0.02	0.02	0.02	0.03
Distance from residential area						-0.22			
Distance from adjacent river			0.004						
Distance from drainage channel			0.006	0.04				-0.03	
Distance from growth centre						0.03			
Soil salinity	-0.08			0.05	0.31	0.11	-0.18	0.17	-0.06
Easting coordinates	0.16		0.07	0.07	0.21	0.05	$2e^{-04}$	-0.17	
Northing coordinates	-0.11	-0.02	0.02		-0.11			0.16	
Population density									
Slope	$-1e^{-04}$		$7e^{-05}$						
ROC	**0.71**	**0.89**	**0.74**	**0.67**	**0.89**	**0.68**	**0.63**	**0.94**	**0.82**
Adjusted odds ratio	**5.23**	**17.82**	**8.10**	**4.28**	**14.38**	**2.96**	**2.07**	**35.74**	**9.81**

LULC 1= Agriculture; LULC 2 = Aquaculture; LULC 3 = Bare land; LULC 4 = Built-up area (urban); LULC 5 = Vegetation with rural settlement; LULC 6 = Waterbody

Table S2. Markov Chain transition probability matrix of LULC change

	LULC class	Agriculture	Aquaculture	Bare land	Built-up area (urban)	Vegetation with rural settlement	Waterbody
Transition probability of 2019 based on the transition matrix of 2005-2010	Agriculture	0.0571	0.4943	0.0713	0.0425	0.2160	0.1189
	Aquaculture	0.0112	0.6845	0.0310	0.0198	0.0492	0.2044
	Bare land / others	0.0983	0.2865	0.2527	0.0227	0.2853	0.0546
	Built-up area (urban)	0.0062	0.1078	0.0121	0.7319	0.0356	0.1063
	Vegetation with rural settlement	0.1226	0.2433	0.1075	0.0246	0.4708	0.0312
	Waterbody	0.0044	0.6815	0.0204	0.0079	0.0236	0.2622
Transition probability of 2030 based on the transition matrix of 2010-2019	Agriculture	0.2296	0.1756	0.2314	0.0189	0.3439	0.0007
	Aquaculture	0.0080	0.7358	0.0724	0.0355	0.0677	0.0806
	Bare land / others	0.0779	0.2742	0.4352	0.0266	0.1790	0.0071
	Built-up area (urban)	0.0007	0.0422	0.0128	0.9310	0.0081	0.0053
	Vegetation with rural settlement	0.0585	0.1897	0.0947	0.0264	0.6257	0.0051
	Waterbody	0.0000	0.7527	0.0569	0.0222	0.0261	0.1421

Table S3. Autocorrelation diagnosis of monthly precipitation

Month	Autocorrelation	Significant
January	-0.12	FALSE
February	0.14	FALSE
March	-0.14	FALSE
April	0.02	FALSE
May	0.18	FALSE
June	-0.01	FALSE
July	0.09	FALSE
August	-0.14	FALSE
September	-0.14	FALSE
October	-0.21	FALSE
November	-0.24	FALSE
December	-0.17	FALSE

Supplementary Figures

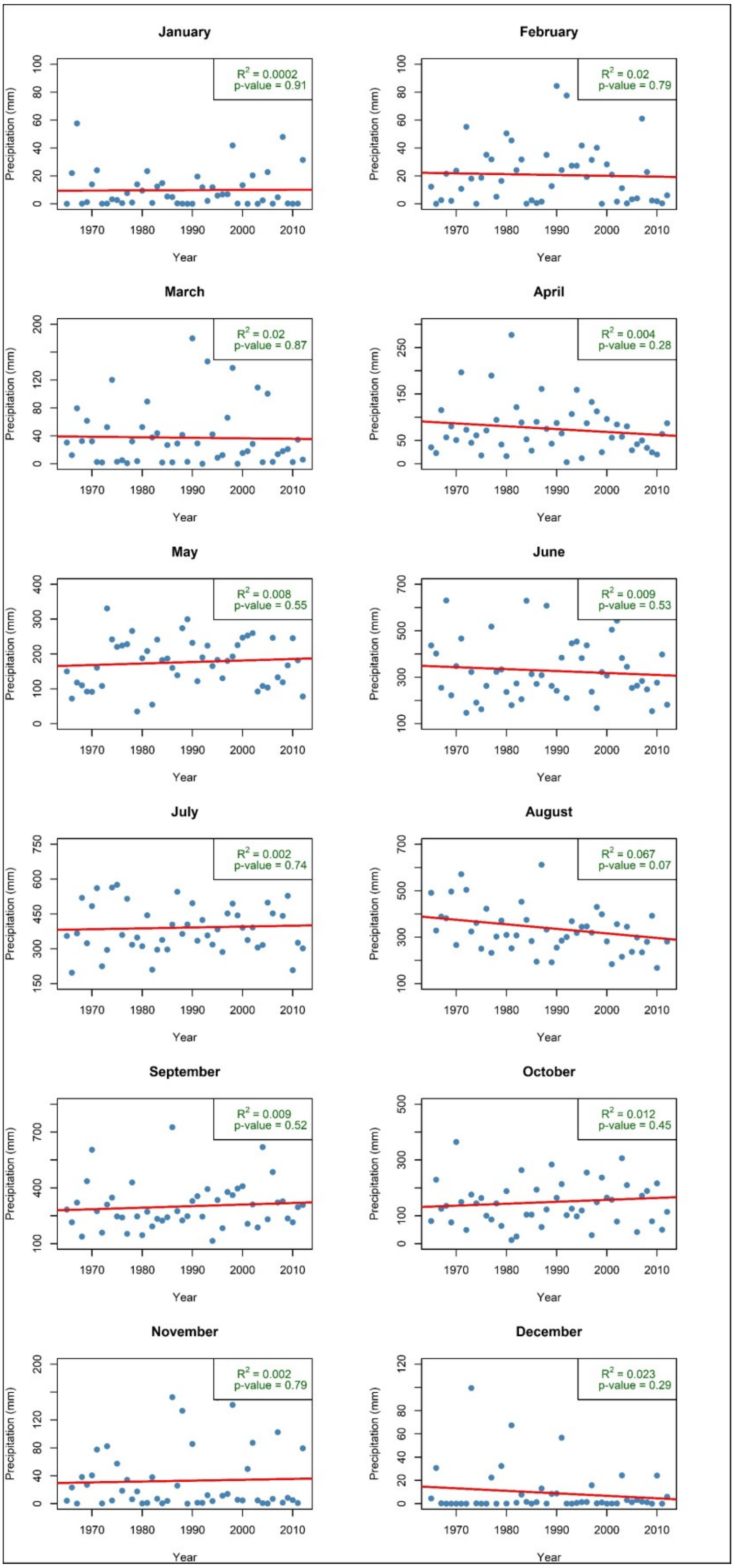

Figure S1. Trend of monthly rainfall from 1965 to 2012

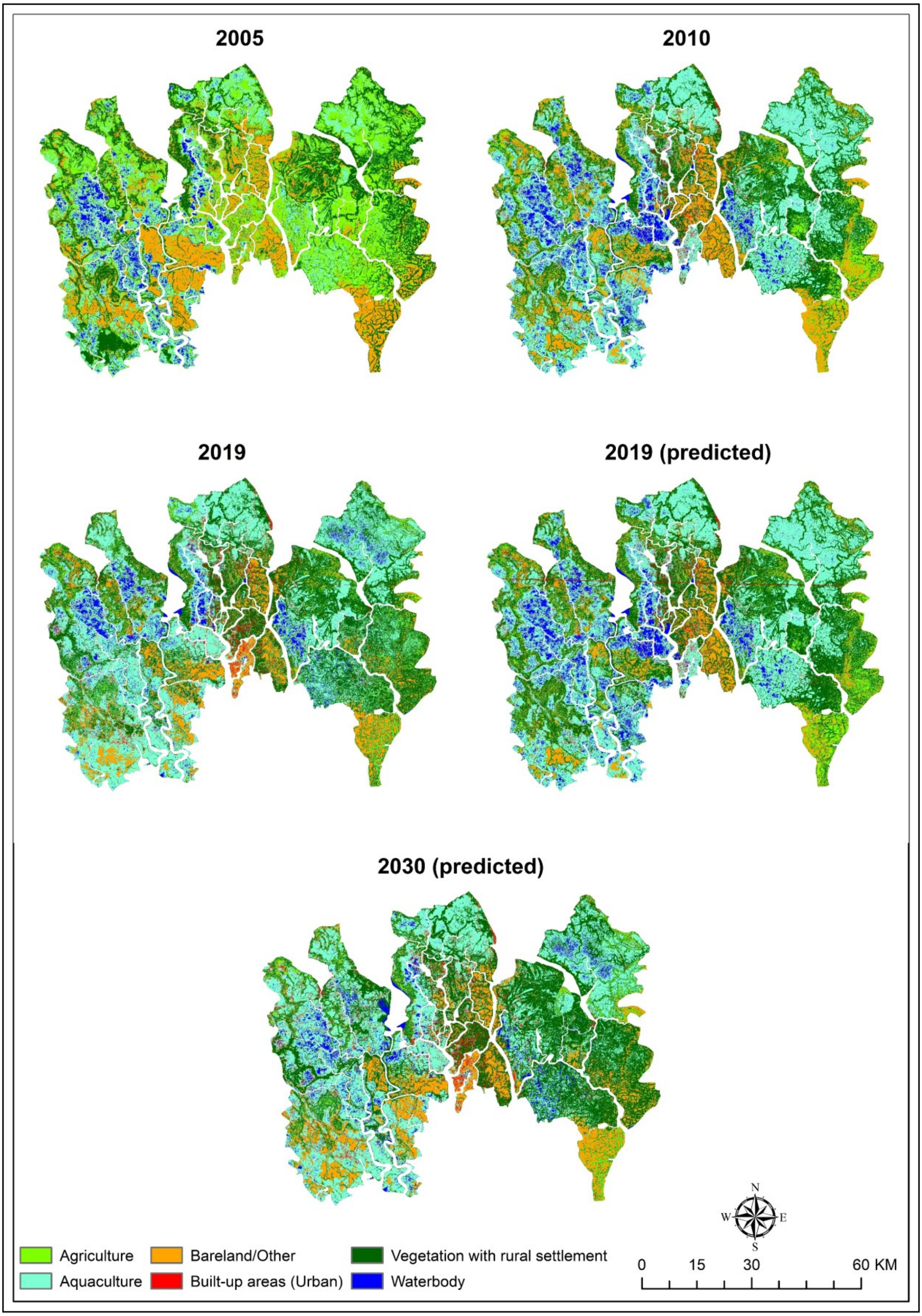

Figure S2. Predicted and observed LULC change between 2005 and 2030

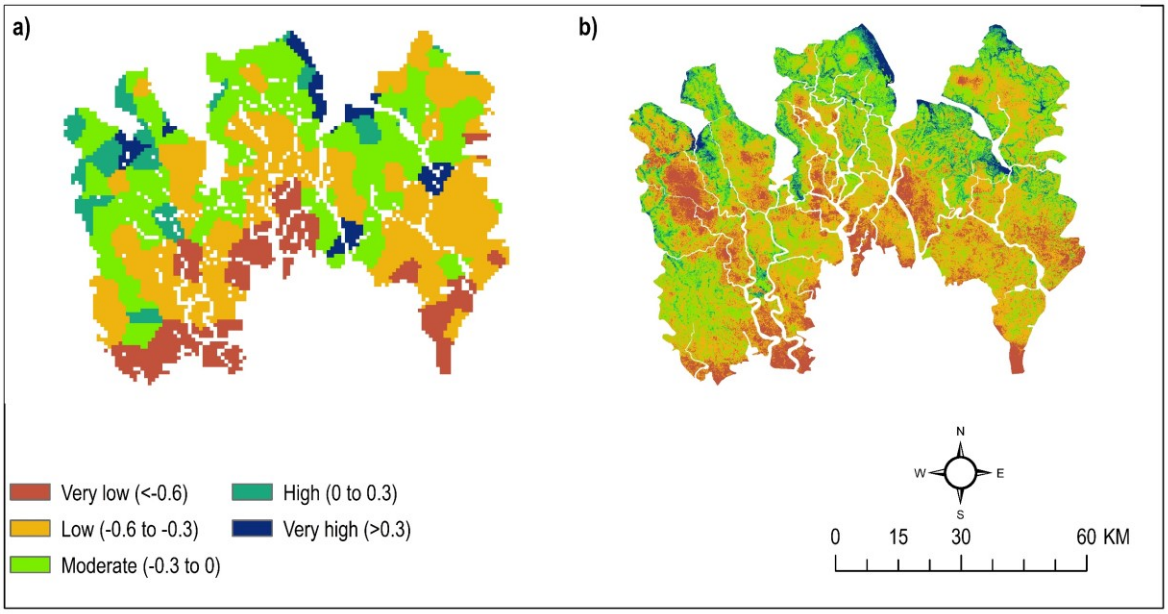

Figure S3. Wealth Index in 2010: a) obtained from Steele et al. (2017); and b) downscaled for this study

References

Steele, J.E., Sundsøy, P.R., Pezzulo, C., Alegana, V.A., Bird, T.J., Blumenstock, J., Bjelland, J., Engø-Monsen, K., de Montjoye, Y.-A., Iqbal, A.M., 2017. Mapping poverty using mobile phone and satellite data. Journal of The Royal Society Interface 14, 20160690.